Search for compact sources of cosmic photons above 200 TeV

D. P. Ciampa, J. Kolodziejczak, K. D. Green, J. Matthews, D. Nitz, D. Sinclair, G. Thornton, and J. C. van der Velde
Department of Physics, University of Michigan, Ann Arbor, Michigan 48109-1120

G. L. Cassiday, R. Cooper, S. C. Corbato, B. R. Dawson, J. W. Elbert, B. E. Fick, D. B. Kieda, S. Ko, D. F. Liebing, E. C. Loh, M. H. Salamon, J. D. Smith, P. Sokolsky, S. B. Thomas, and B. Wheeler
Department of Physics, University of Utah, Salt Lake City, Utah 84112
(Received 16 August 1991)

From April 1988 to February 1990 we used a two-level array of scintillators to search in the cosmic radiation for compact sources of γ rays above 200 TeV. Counters on the surface measured the size and direction of extensive air showers while counters buried 3 m below ground measured their muon content. Showers induced by γ rays are expected to have many fewer muons than those initiated by hadrons so the selection of muon-poor showers should greatly reduce the background of hadronic showers. Three objects, Cygnus X-3, the Crab nebula, and Hercules X-1, were examined in detail. Searches were made on short and long time scales and source periodicity was used, where applicable, to enhance any possible signals. We found no evidence for any compact sources.

PACS number(s): 98.70.Rz

I. INTRODUCTION

In the past decade many observations of compact sources of cosmic rays at ultrahigh energies (UHE) ($>10^{14}$ eV) have been reported. The x-ray binary system Cygnus X-3 was the first such source [1]. Other observers subsequently reported on this object and many others, most notably the Crab Nebula and another x-ray binary Hercules X-1. These results have been extensively reviewed in the literature [2–5]. Many reputed UHE γ-ray sources have been identified as x-ray emitters, and GeV γ-rays from the Crab and Vela pulsars have been reported by the SAS-2 [6] and COS-B [7] satellites. Unlike observations at lower energies in which the techniques used to detect the radiation favored γ rays, the nature of the UHE radiation is uncertain. Indeed, some experiments have indicated that a new form of neutral radiation was involved.

There is no compelling evidence of steady nor of regularly repeating episodic UHE emission from any source. Many experiments which have reported positive detection of a source find that the magnitude of the signal is not large enough by itself to give a statistically significant result; additional criteria such as correlation with orbital or pulsar periods are required in order to reduce the cosmic-ray background. Furthermore, several experiments which have looked for reported sources have not found them. Indeed, it has been argued that the evidence is insufficient to conclude that there are *any* sources of UHE γ rays [8].

The significance of the discovery of compact sources of UHE γ rays is that such objects may be the sites of UHE cosmic-ray production and acceleration. The behavior of the cosmic-ray spectrum near the so-called "knee" ($\simeq 2\times 10^{15}$ eV) is not well understood. Compact objects may provide a new component of cosmic rays in this region. If UHE γ rays do exist and are produced by hadronic interactions near the source, the power output of these sources in UHE cosmic rays would be enormous. For example, Hillas [9] has pointed out that if the Kiel observations of Cygnus X-3 are taken at face value, then only a few such sources are required to account for all cosmic rays observed above 10^{16} eV.

We have searched for compact sources of UHE γ rays using the muon content of extensive air showers to distinguish γ-ray-induced events. Measurements of muons in extensive air showers sensitively discriminates γ rays from the ordinary cosmic-ray background since muons are copiously produced in hadronic air showers but are relatively rare in showers initiated by γ rays. This effect can be simply understood by the large size of the pair-production cross section relative to that of pion photoproduction. The validity of this approach is based on the assumption that UHE γ rays have interaction properties which can be extrapolated from lower energies.

Because the observations of Cygnus X-3 by the Kiel [10] group and others [2–5] were made with showers which were not muon poor, speculation has arisen that the muon content of UHE photon-induced showers approaches that of showers induced by hadrons. However, theoretical attempts to significantly increase the number of muons in γ-ray air showers without introducing radically new physics have failed [11]. The experimental evidence remains inconclusive. At TeV energies, the Whipple Collaboration, while not measuring muons, reported that γ rays from the Crab Nebula have other characteristics expected from standard electrodynamics [12]. On the other hand, other sources observed with less statistical significance by Whipple do not exhibit those characteristics (see Ref. [5]). Nevertheless, we believe the con-

ventional picture of γ-ray interactions remains the best framework in which to attempt to observe UHE γ rays.

In an earlier paper [13] we reported on a search for γ rays from Cygnus X-3. The results reported here are from a data set that is approximately 25% larger. The angular aperture used in this work is a square 5.2° on a side, centered on the source. In the previous work we used a circle of 3° radius. The results reported here and the techniques used to obtain them are described in greater detail in two theses [14].

II. DESCRIPTION OF THE EXPERIMENT

The Utah-Michigan array was operated between January 1988 and February 1990 at the site of the Fly's Eye installation in Dugway, Utah (40° N, 113° W, atmospheric depth 870 g/cm^2). As shown in Fig. 1, there were 33 counterstations on the surface distributed within a circle of 100-m radius, and 512 counters arranged in eight patches buried 3 m underground. The surface counters were used to measure the size and direction of each shower while the buried counters sampled the muons. A counterstation on the surface had an area of 1.5 m^2 and consisted of four slabs of scintillator, each viewed by two photomultiplier tubes (PMTs). A patch of buried counters contained 64 sheets of scintillator, each 2.5 m^2 in area and viewed by a single 5-in. PMT at its center. Measurements [15] with overlapping scintillators showed that a typical buried counter detected muons with an efficiency of 93%. The experiment began operating with the inner four patches of muon counters. The outer four patches were brought on line during the first half of the run. By January 1989 all eight patches were operating, having a total area of 1280 m^2.

An event was recorded when at least 7 surface stations and 15 or more surface counters reported hits within 2 μs. The buried array did not participate in the event trigger, so there was no bias with regard to the muon content of recorded showers. For each surface station we recorded which counters were hit, the time of the first hit, and the total energy deposited in the four counters in that station. These data were used to calculate the direction and total charged-particle size N at the ground for each shower.

Size spectra of showers which triggered the array are shown in Fig. 2. The onset of the trigger caused some loss of showers with $N < 5 \times 10^4$. Saturation of the surface stations caused an underestimation of showers with $N > 10^6$. In the region between these limits the size spectrum fits approximately a power law with a spectral index equal to -1.5. The sample used in this analysis includes only those showers for which $N > 10^4$ and whose cores lay within 100 m of the center of the array. The angular resolution was measured to be $\delta\theta = 3°$, where $\delta\theta$ would contain 71% of the events for a point source. Systematic pointing error was measured to be less than 0.3°. The methods used to determine the sizes and directions of showers and to measure the angular resolution are described in another paper [16].

The muons associated with each shower were sampled by the buried counters. We recorded the arrival times of the first hit for each of the buried counters but not the number of particles hitting an individual counter. The time window for accepting pulses from the muon counters was ± 55 ns for the inner four patches and ± 100 ns for the outer four, relative to the arrival time of the shower front at the buried counters as determined by the surface array. We found the total muon size N_μ by a maximum likelihood fit, which compared the hits and misses to the lateral distribution function for muons given by Greisen [17]. In making the fit we used the core location determined by the surface array. Size spectra of the muons in showers which triggered the array are shown in Fig. 2(b). The onset of the trigger provided by the surface array caused some loss of showers with $N_\mu < 10^4$.

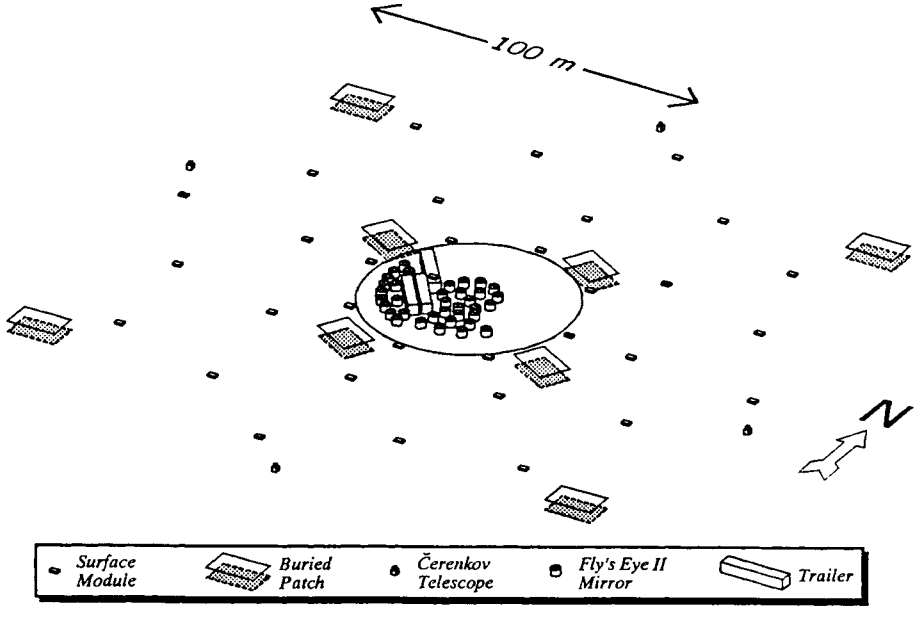

FIG. 1. Elevated view of the Utah-Michigan array. The shaded rectangles indicate eight 64-counter muon patches. The smaller rectangles show positions of the 33 units of the surface array. The Fly's Eye II installation and electronics trailers are shown at the center.

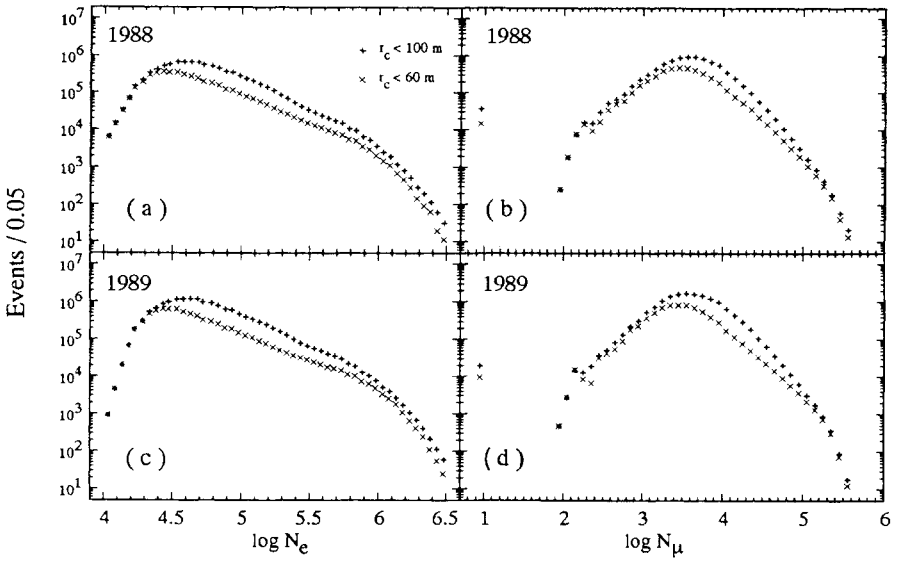

FIG. 2. Size spectra of showers recorded in 1988 and 1989. (a) and (c) refer to the number of electrons in showers as measured by the counters on the surface, while (b) and (d) refer to the number of muons as measured by the buried counters. The quantity r_c is the distance of a shower's core from the center of the array.

We assumed that the muon component of showers of all sizes and slant angles could be fitted to a single lateral distribution function by adjusting only the parameter N_μ. This assumption is justified by the data. In Fig. 3 we show lateral distributions measured by summing hits in all the buried counters over many showers. These are almost the same for the two groups of showers: (a) showers within 5° of the zenith and (b) showers slanting at more than 30° to the zenith. They agree with the lateral distribution function of Greisen [17] (solid lines) to within 10%. They also demonstrate that electromagnetic *punch through* to the muon counters is negligible. Punch through would reveal itself as an excess of hits near the cores of showers. The data in Fig. 3 show that this excess is less than 2% of the detected muons. The measurement of punchthrough is described in more detail in Ref. [16].

III. SELECTION OF MUON-POOR SHOWERS

Our measurements show that the average number of muons associated with ordinary cosmic-ray showers depends on the total particle size at the surface (N) and zenith angle θ in the following way:

$$\langle \log_{10} N_\mu \rangle = a + b \sec\theta + c \log_{10} N \ . \quad (1)$$

The coefficients in expression (1) are determined separately for each data run of about 24 h, since the pressure of the atmosphere varies with local weather conditions. Average values for a, b, and c are -0.98, 0.62, and 0.82, respectively. The dependence on zenith angle arises because the electron and muon components of the shower develop differently as the shower progresses. Simulations of showers show that for a fixed energy of primary (hadronic) cosmic ray, the number of electrons at the ground decreases rapidly with increasing zenith angle while the number of muons decreases relatively slowly.

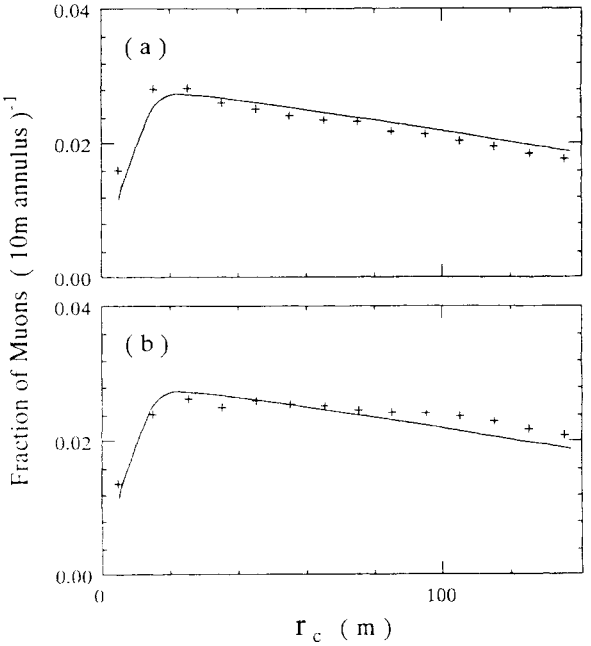

FIG. 3. Lateral distributions of muons as measured by accumulated hits in the buried counters (a) for showers within 5° of the zenith and (b) for showers slanting at more than 30° to the zenith. The points represent the fraction of the total number of buried counter hits accumulated in rings of width 10 m and distances r_c from the shower axis. Error bars are slightly less than the size of the plot symbols. The solid curves are calculated from the lateral distribution function of Greisen with a 10-m smearing of the function to account for errors in measuring positions of shower cores. The distributions contain showers with $N > 3\times10^4$. Some punchthrough is evident as a small excess of hits close to the core. The amount of punchthrough decreases at larger zenith angles due to increased absorption in air and earth.

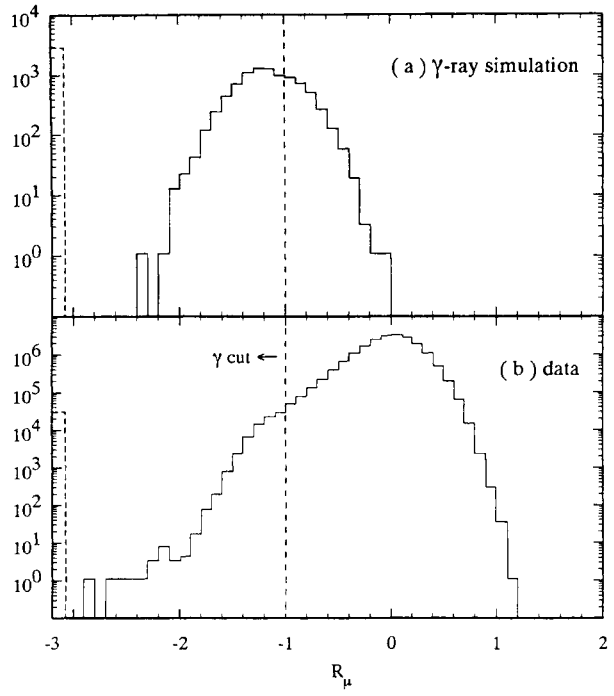

FIG. 4. Distribution of the relative muon size R_μ [Eq. (2)] for (a) simulated γ-ray showers and (b) data. 80% of simulated γ-ray events have $R_\mu < -1.0$ (shown by the dotted line). In each figure, showers with no recorded muons are plotted as underflows in the dashed bin at the left.

The muon content of individual showers fluctuates about the mean value given by expression (1). We define the *relative muon size* R_μ of individual showers as

$$R_\mu \equiv \log_{10} N_\mu - \langle \log_{10} N_\mu \rangle \ . \tag{2}$$

The distribution of this quantity is shown in Fig. 4(b). Fluctuations in R_μ correspond to a full width at half maximum of 0.52. Showers initiated by γ rays are expected to have far fewer muons than ordinary hadronic cosmic rays and, consequently, will have smaller R_μ values. The distribution of R_μ for a simulated sample of γ-ray events is shown in Fig. 4(a).

We can enhance the γ-ray content of the data by retaining only those showers which have R_μ below some selected value. There is an optimum value of R_μ for which a large fraction of ordinary cosmic rays are removed and a relatively small number of γ-ray showers are rejected. We obtain this value by maximizing the quantity $\alpha_\gamma/\sqrt{\alpha_a}$, where α_γ represents the fraction of γ-ray showers passing a given cut in R_μ, while α_a is the corresponding fraction for all showers. The quantity α_γ is obtained by simulating the array's response to γ-ray showers using simulations of Halzen *et al.* [11] to provide the muon content of γ-ray showers, while α_a is derived from the data shown in Fig. 4. The result of this optimization is shown in Fig. 5. It indicates that a cut in R_μ in the range -1.0 to -1.4 should result in a signal enhancement $\alpha_\gamma/\sqrt{\alpha_a} \simeq 12$.

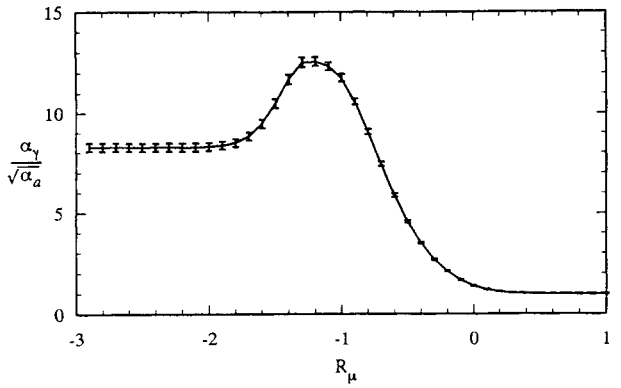

FIG. 5. The quantity $\alpha_\gamma/\sqrt{\alpha_a}$ is shown vs R_μ, which is a measure of how muon poor a shower is. $\alpha_\gamma/\sqrt{\alpha_a}$ is a measure of how well γ-ray-induced showers are separated from all others showers.

IV. AREA SEARCH FOR COMPACT SOURCES

The data used in this section were taken from 377 live days collected between April 4, 1988 and January 1, 1990. They consist of 2.4×10^7 showers with $N > 10^4$. To search for compact sources of γ rays we divided the surface of the celestial sphere into bands of declination 5.2° wide. Each declination band was divided into an integral number of bins which were as nearly square as possible. The single exception to this procedure was the bin at the pole which was a circle of radius 3°. Our angular resolution is such that each square should contain 70% of the γ rays from a point source located at its center. The search was carried out by offsetting the grid by half a square in both declination (DEC) and right ascension (RA), so that the area was oversampled by a factor 4.

The showers were divided into several groups which were examined separately. The criteria used were shower size, core location relative to the center of the array, and muon content. Also, data taken during 1989 were examined separately since all eight muon patches were in use for that year, while during 1988 the number of patches grew from four to eight. After subtraction of background, using the method described below, each bin was examined for evidence of a significant surplus. Some examples of excesses above 3σ were found, but not more than would be expected from normal fluctuations. This is illustrated in Fig. 6, where we show the frequency distribution of deviations from the background for showers with $R_\mu < -1.25$ collected in 1989. Locations showing excesses of muon-poor showers above 3σ are listed in Table I. There were no locations with excesses above 3.5σ. To set limits on the γ-ray flux, we need to know the exposure of the array. The exposure of the array and the threshold energy depend on the declination of the source. The procedure for calculating these quantities is described in Sec. V. The γ-ray flux corresponding to a 3.5σ excess is shown in Fig. 7 as a function of the declination of the source.

The method used to estimate the backgrounds for the various subsets of data can be understood by considering

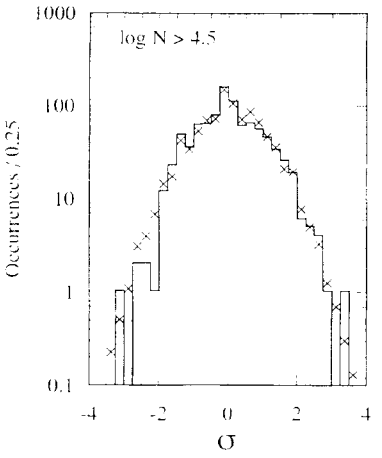

FIG. 6. Distribution of the differences between muon-poor showers ($R_\mu < -1.25$) and background, in standard deviations σ, for the ~800 elements of the celestial sphere into which the data were subdivided. The ×'s represent the distribution expected due to normal fluctuations. They were calculated as follows. For each element of RA and DEC we calculated a Poisson probability distribution with a mean corresponding to the background in that element. To each integer value of this Poisson distribution we assigned an equivalent value of a Gaussian distribution in units of σ. We then combined the Poisson distributions for all elements of RA and DEC. This procedure was used because the number of events in many bins was too small for Gaussian statistics to be applicable.

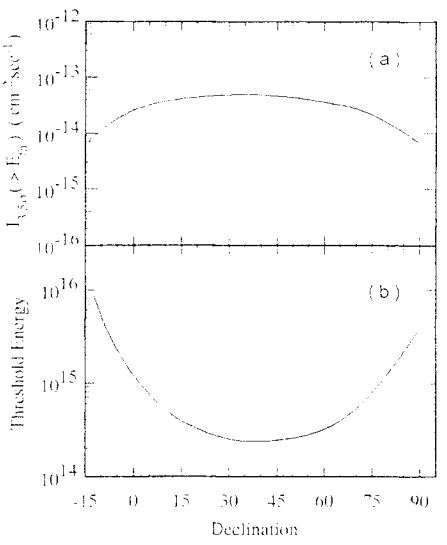

FIG. 7. Results of a scan of the northern celestial hemisphere for compact sources of γ rays. The excesses of muon-poor showers above background follow a Poisson distribution with nothing exceeding 3.5σ. The integral flux corresponding to this excess is shown in (a). The corresponding energy threshold, defined as the energy at which the response of the array reaches 25% of its maximum value, is given in (b).

a particular location on the celestial sphere. As this point revolves around the celestial pole, the flux of cosmic rays which passes our cuts and comes from that location increases in intensity as the point rises toward the zenith and decreases as it sets. Let us suppose there is a source at this location. To calculate the background for this source, we sum the times when the detector is on and the source is at a particular hour angle, weighted by the rate of cosmic rays corresponding to that hour angle and declination. We do this by keeping track of the detectors recording rate throughout its lifetime, since the rate of cosmic rays varies with changes in barometric pressure and the triggering conditions of the array. The backgrounds thus obtained for each element of RA and DEC are then normalized to the data in each strip of DEC.

TABLE I. Directions from which showers with $R_\mu < -1.25$ exceed background by more than 3σ. The data were collected during 1988 and 1989. A few locations with excesses above 3σ are to be expected due to random fluctuations.

Shower size	RA (deg)	DEC (deg)	Observed	Background	Excess (σ)
$>10^4$	104.3	−15.4	3	0.1	3.5
	166.8	17.9	100	68.9	3.5
$>10^{4.5}$	264.8	15.4	51	32.2	3.0
	335.0	23.0	76	52.0	3.1
$>10^5$	8.0	15.4	7	1.4	3.4
	51.8	33.3	12	3.9	3.2

V. STUDY OF SELECTED SOURCE CANDIDATES

Three candidates were selected for study. These were Cygnus X-3, the Crab Nebula, and Hercules X-1. The data were collected between April 4, 1988 and February 20, 1990. They include showers with $N > 3\times10^4$ coming from a square patch of the sky 5.2° on a side and centered on the suspected source. This should include 70% of the γ rays from a point source. We have previously reported [13] on one of these objects, Cygnus X-3. The results presented here involve a slightly larger sample of data.

A. Limits on the time-averaged radiation

To measure the flux from a source or to set a limit we need to know the exposure of the array to the source. As the source rises and sets, the solid angle subtended by the array changes, being a maximum when the source is at its highest point in the sky and dropping to zero when it sets. Also, the thickness of atmosphere between the array and the source changes, so showers of a given energy arrive at different stages of development, requiring that the relation between shower size and energy be changed with the zenith angle of the source. These effects are included in the computation of a function $A(E,t)$ for each source. Here E is the energy of the primary photon, t is time, and $A(E,t)$ represents the area of the array seen by the source. Thus the number of photons with energies between E and $E+dE$ detected by the array is given by

$$dN_\gamma = kE^{-\beta}\int_0^T A_s(E,t)dt\,dE\ ,$$

where the quantity $kE^{-\beta}$ represents the flux of γ rays from the source incident on the earth. For each source we calculate a quantity $\mathcal{E}_s$, the exposure of the array,

TABLE II. Showers with $N > 3\times10^4$ coming from the directions of suspected compact sources of γ rays are compared with the background. The observed showers come from a solid angle equal to 8.2×10^{-3} sr, which should include 70% of the γ rays from a point source.

Source	Exposure (10^6 m^2 d)	Threshold[a] (10^{14} eV)	R_μ	α_γ	Observed showers	Expected background	Excess 90% C.L.	Flux (cm^{-2}s^{-1})
Cyg X-3	3.35	2.4	All	1.0	49915	50260	<217	$<1.0\times10^{-13}$
			<-1.0	0.8	296	273	<47	$<2.3\times10^{-14}$
Crab	2.72	3.0	All	1.0	30422	30255	<410	$<2.4\times10^{-13}$
			<-1.0	0.8	156	163	<19	$<1.1\times10^{-14}$
Her X-1	3.19	2.4	All	1.0	47788	47670	<441	$<2.2\times10^{-13}$
			<-1.0	0.8	281	259	<46	$<2.3\times10^{-14}$

[a]Defined as the energy at which the response of the array reaches 25% of its maximum value.

which is defined as

$$\mathcal{E}_s\int_{E'}^{\infty}kE^{-\beta}dE\equiv\int_0^{\infty}kE^{-\beta}\int_0^{T}A_s(E,t)dt\,dE\ .$$

Here E' is the energy at which the array becomes sensitive to showers. Because of large fluctuations in the development of showers, the response of the array turns on rather slowly with energy, so the choice of a threshold is somewhat arbitrary. The energy threshold for each source given in Table II is chosen to be the energy at which the response of the array reaches 25% of its maximum values. But the values of exposure and threshold are correlated, so the result of our measurement does not depend on the choice. What we measure, or set a limit on for each source, is the scale of an assumed differential energy spectrum, which is then expressed as a point on the corresponding integral spectrum. For the Crab we used -2.4 for the index of the differential energy spectrum based on lower-energy results from Whipple [12]. For Cygnus X-3 and Hercules X-1 we used -2.0, a value inferred from measurements at lower energies [2–5]. The preceding method for calculating the exposure of the array to a given source is described in more detail in Ref. [13].

To estimate the backgrounds for these data we used the following method. In the horizontal coordinate frame we took a strip of declination centered on the source, and we populated each element of hour angle along this strip with a number equal to the rate of cosmic rays which passed our cuts and came from that part of the sky. Actually, since the flux of cosmic rays varies slightly with changes in barometric pressure we accumulated a separate hour-angle distribution for each data run of approximately 24 h. Using these distributions we integrated the contributions from each element of hour angle weighted by the detector's on time when the source was at that hour angle.

The results are shown in Table II. The quantity α_γ represents the fraction of γ-ray showers that should survive the cut in R_μ. The measured limits are integral fluxes above the stated thresholds. Confidence limits were calculated using Poisson statistics with background present [18].

B. Search for short-term bursts

We have searched the data for bursts on time scales of 1.2 h and 1 d (actually 1 full transit of the source). The expected cosmic-ray backgrounds for these short segments were measured in precisely the same way as for the full data set. Standard deviations calculated from the formula of Li and Ma [19] were obtained for each time segment using the observed events and expected background. The distributions of standard deviations showed no particularly unusual bursts for any of the three suspected sources. Using muon-poor showers, typical flux limits (90% C.L.) for 1.2-h bursts and 1-d bursts are 8×10^{-12} cm^{-2}s^{-1} and 2×10^{-12} cm^{-2}s^{-1}, respectively. If the muon-poor criterion is removed, the limits are a factor 5 higher.

C. Search for modulated signals

We have searched the data for periodicity in the rate of showers from each of the three sources corresponding to that which they exhibit in the x-ray region. We find no evidence for such effects. The results are shown in Fig. 8. For both ordinary showers and muon-poor showers ($R_\mu<-1.0$), the phasograms using the published [20] ephemerides are in good agreement with the backgrounds.

In estimating the backgrounds we treated the Crab differently from the other sources. The period of the Crab pulsar (33 ms) is so short that there is surely no correlation between its phase and the daily fluctuations in intensity due to the rising and setting of the source. Thus, for the Crab, we drew a flat background on the light curve. To calculate the backgrounds for the other sources we took the strip of declination centered on the source and averaged the phase distributions of the events in the two bins adjacent to the source in RA.

VI. CONCLUSIONS

We saw no evidence for any sources of γ rays in our energy range. Results for the three candidates that we examined in detail were negative, even when timing criteria were applied. In an earlier paper [13] we summarized the published data on Cygnus X-3. Our limit, based

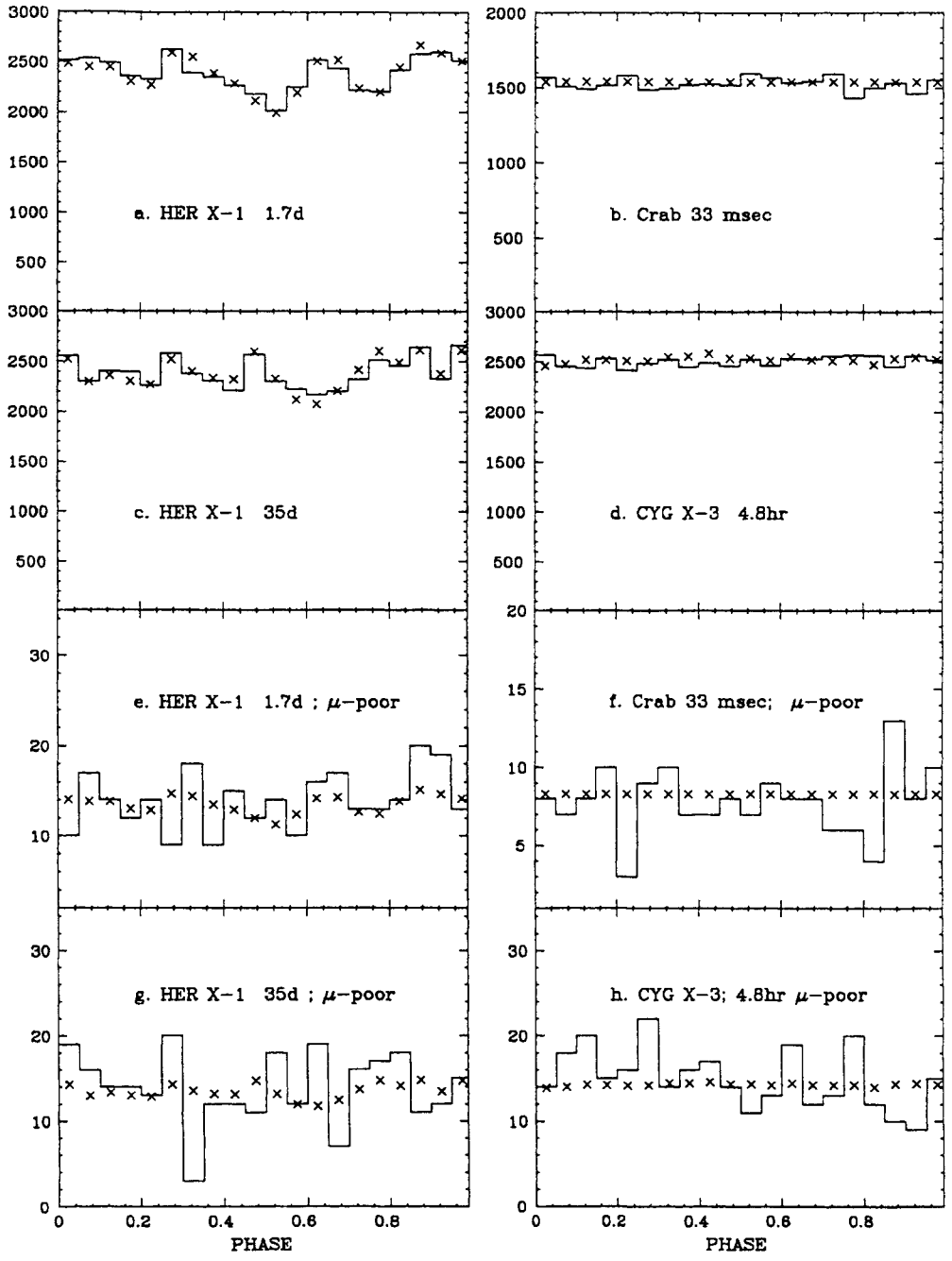

FIG. 8. Phasograms for (a) the 1.7-d period of Hercules X-1, (b) the 0.0334-s period of the Crab pulsar, (c) the 35-d period of Hercules X-1, and (d) the 4.8-h period of Cygnus X-3. (e)–(h) are the corresponding light curves for muon-poor showers ($R_\mu < -1.0$). The $\times$'s represent the backgrounds.

on muon-poor showers, falls well below the intensities of previous sightings when these are adjusted to correspond to our energy threshold.

Our limit for steady emission from the Crab nebula is 1.1×10^{-14} cm^{-2}s^{-1}, $E > 300$ TeV. This source has been observed as a steady emitter of γ rays at energies of ~ 1 TeV by the Whipple group [12]. Their results show a differential energy spectrum which falls as $E^{-2.4}$. If we extrapolate their measurement to the energy of our experiment, we would expect a flux of $\sim 5\times10^{-15}$ cm^{-2}s^{-1}. We point out, however, that the exponent of the energy measured in the Whipple experiment has an error of ± 0.25. Our limit tends to rule out a spectrum harder than $E^{-2.3}$ extending to our energy range.

Hercules X-1 has never been observed as a steady source of γ rays, but bursts of radiation have been reported. The Cygnus Array [21] observed a burst in July of 1986 with a duration of approximately 1 h at an intensity of 2×10^{-11} cm^{-2}s^{-1} at energies above 100 TeV. Working at much lower energies (~ 1 TeV), a Cherenkov

detector on Mount Haleakala [22] observed a burst of ~ 15 min duration in June of 1986, and in May of the same year a similar detector on Mount Hopkins [23] observed a 15-min burst. The estimated intensities in these observations were 5×10^{-10} and 2×10^{-10} $cm^{-2}s^{-1}$, respectively. Our limit of 8×10^{-12} $cm^{-2}s^{-1}$ for 1.2-h bursts from Hercules X-1 lies just below the intensity observed by the Cygnus Array after allowing for the different energy thresholds of the two arrays. However, their observations involved showers which were not muon poor, and were not contemporaneous with ours, so the two results are not in contradiction. The signals observed by the Cherenkov detectors were at an energy much lower than ours, so our result does not challenge these measurements.

ACKNOWLEDGMENTS

The authors gratefully acknowledge the help and support of Col. J. A. Van Prooyen and the staff of Dugway Proving Grounds. This work was supported in part by the U.S. Department of Energy and the National Science Foundation.

[1] M. Samorski and W. Stamm, Astrophys. J. **268**, L17 (1983).
[2] D. E. Nagle, T. K. Gaisser, and R. J. Protheroe, Annu. Rev. Nucl. Part. Sci. **38**, 609 (1988).
[3] T. C. Weekes, Phys. Rep. **160**, 1 (1988).
[4] P. M. Chadwick, T. J. L. McComb, and K. E. Turver, J. Phys. G **16**, 1773 (1990).
[5] D. J. Fegan, in *Proceedings of the 21st International Cosmic Ray Conference,* Adelaide, Australia, 1990, edited by R. J. Protheroe (Graphic Services, Northfield, South Australia, 1990), Vol. 11, p. 23.
[6] R. C. Hartman *et al.*, Astrophys. J. **230**, 597 (1979).
[7] H. A. Mayer-Hasselwander *et al.*, Astron. Astrophys. **105**, 164 (1982).
[8] J.-M. Bonnet-Bideaud and G. Chardin, Phys. Rep. **170**, 325 (1988).
[9] A. M. Hillas, Nature (London) **312**, 50 (1984).
[10] M. Samorski and W. Stamm, in *Proceedings of the 18th International Cosmic Ray Conferences,* Bangalore, India, 1983, edited by N. Durgaprasad *et al.* (TIFR, Bombay, 1983), Vol. 11, p. 244.
[11] F. Halzen *et al.*, Phys. Rev. D **41**, 342 (1990).
[12] G. Vaccanti *et al.*, Astrophys. J. **377**, 467 (1991).
[13] D. Ciampa *et al.*, Phys. Rev. D **42**, 281 (1990).
[14] J. J. Kolodziejczak, Ph.D. thesis, University of Michigan, 1990; D. P. Ciampa, Ph.D. thesis, University of Michigan, 1991.
[15] D. Sinclair, Nucl. Instrum. Methods A **278**, 583 (1989).
[16] J. Matthews *et al.*, Astrophys. J. **375**, 202 (1991).
[17] K. Greisen, Annu. Rev. Nucl. Sci. **10**, 63 (1960).
[18] O. Helene, Nucl. Instrum. Methods A **212**, 319 (1983); Particle Data Group, G. P. Yost *et al.*, Phys. Lett. B **204**, 1 (1988).
[19] T. Li and Y. Q. Ma, Astrophys. J. **272**, 317 (1983).
[20] For Cygnus X-3 we used M. van der Klis and J. M. Bonnet-Bidaud, Astron. Astrophys. **214**, 203 (1989). For the Crab we used A. G. Lyne and R. S. Pritchard (private communication). For the 1.7-d period of Hercules X-1 we used J. E. Deeter, P. E. Boynton, and S. H. Pravdo, Astrophys. J. **247**, 1003 (1981), and for the 35-d period of Hercules X-1 we used H. Ogelman, Astron. Astrophys. **172**, 79 (1987).
[21] B. L. Dingus *et al.*, Phys. Rev. Lett. **61**, 1906 (1988).
[22] L. K. Resvanis *et al.*, Astrophys. J. **328**, L9 (1988).
[23] R. C. Lamb *et al.*, Astrophys. J. **328**, L13 (1988).

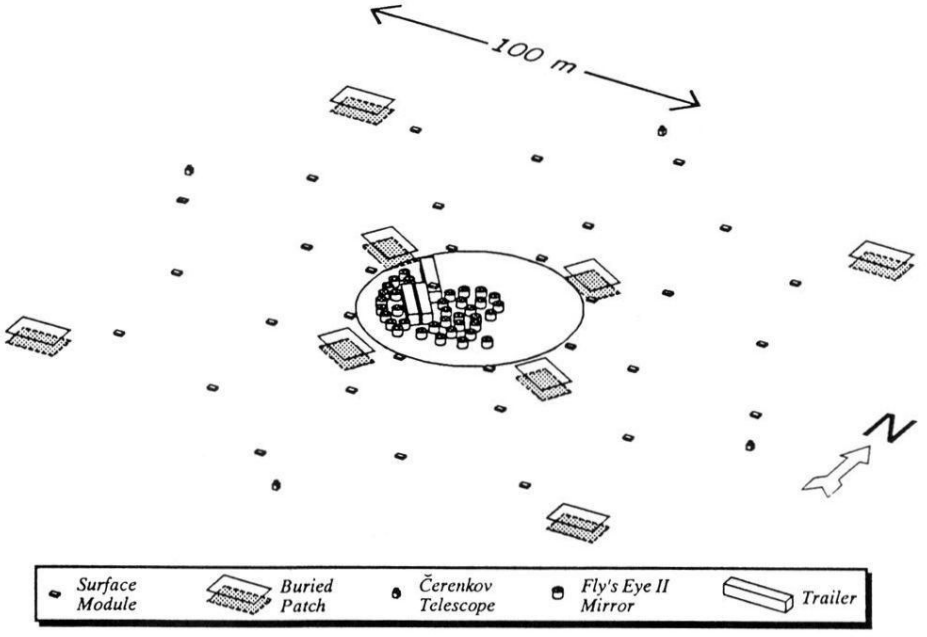

FIG. 1. Elevated view of the Utah-Michigan array. The shaded rectangles indicate eight 64-counter muon patches. The smaller rectangles show positions of the 33 units of the surface array. The Fly's Eye II installation and electronics trailers are shown at the center.